Received: 25 May 2020 | Accepted: 13 October 2020

DOI: 10.1111/pce.13937

ORIGINAL ARTICLE

Plant, Cell & Environment WILEY

Dying by drying: Timing of physiological stress thresholds related to tree death is not significantly altered by highly elevated CO_2

Marielle Gattmann | Benjamin Birami | Daniel Nadal Sala | Nadine Katrin Ruehr

Institute of Meteorology and Climate Research – Atmospheric Environmental Research, Karlsruhe Institute of Technology KIT, Garmisch-Partenkirchen, Germany

Correspondence
Marielle Gattmann, Karlsruhe Institute of Technology KIT, Institute of Meteorology and Climate Research – Atmospheric Environmental Research, 82467 Garmisch-Partenkirchen, Germany.
Email: marielle.gattmann@kit.edu

Funding information
Deutsche Forschungsgemeinschaft, Grant/Award Numbers: Emmy Noether Program (RU 1657/2-1), German-Israeli project cooperation program (CSCHM; Helmholtz Association, Grant/Award Number: research program ATMO

Abstract

Drought-induced tree mortality is expected to occur more frequently under predicted climate change. However, the extent of a possibly mitigating effect of simultaneously rising atmospheric [CO_2] on stress thresholds leading to tree death is not fully understood, yet. Here, we studied the drought response, the time until critical stress thresholds were reached and mortality occurrence of *Pinus halepensis* (Miller). In order to observe a large potential benefit from eCO_2, the seedlings were grown with ample of water and nutrient supply under either highly elevated [CO_2] (eCO_2, *c.* 936 ppm) or ambient (aCO_2, *c.* 407 ppm) during 2 years. The subsequent exposure to a fast or a slow lethal drought was monitored using whole-tree gas exchange chambers, measured leaf water potential and non-structural carbohydrates. Using logistic regressions to derive probabilities for physiological parameters to reach critical drought stress thresholds, indicated a longer period for halving needle starch storage under eCO_2 than aCO_2. Stomatal closure, turgor loss, the duration until the daily tree C balance turned negative, leaf water potential at thresholds and time-of-death were unaffected by eCO_2. Overall, our study provides for the first-time insights into the chronological interplay of physiological drought thresholds under long-term acclimation to elevated [CO_2].

KEYWORDS
drought, net C balance, non-structural carbohydrates, respiration, tree mortality, turgor loss, water-use-efficiency

1 | INTRODUCTION

Rising temperatures, changing precipitation patterns, more frequent as well as more severe extreme weather events are well-known projections of global climate change (Dai, 2013; Huang, Yu, Guan, Wang, & Guo, 2016; IPCC, 2014; Reichstein et al., 2013). In the last two decades, many experimental as well as modeling approaches have been broaching the issue of how climate affects forest ecosystems (Hlásny et al., 2017; Hui, Deng, Tian, & Luo, 2017) as this research topic significantly gained in importance and acuteness (Liu et al., 2017; Nabuurs, Hengeveld, van der Werf, & Heidema, 2010; Sáenz-Romero et al., 2017) due to an increase in reports of drought-induced tree mortality events in forest ecosystems around the globe (Allen et al., 2010; Allen, Breshears, & McDowell, 2015; Anderegg,

This is an open access article under the terms of the Creative Commons Attribution License, which permits use, distribution and reproduction in any medium, provided the original work is properly cited.
© 2020 The Authors. Plant, Cell & Environment published by John Wiley & Sons Ltd.

Anderegg, Kerr, & Trugman, 2019; Bréda, Huc, Granier, & Dreyer, 2006; Fensham & Holman, 1999; Phillips et al., 2010). In light of these observations and the regulatory function of forests within the global carbon and water cycle, the ability to assess and attribute tree death is of great interest (Adams et al., 2010). In this context, increasing atmospheric [CO_2] (C_a), a main driver of global climate change is considered as a possible antagonistic factor that may mitigate some of the adverse impacts of climate alterations on tree mortality to a certain extent (Brodribb, Powers, Cochard, & Choat, 2020).

During drought events, stomatal closure reduces water loss and simultaneously impairs CO_2 diffusion (Hsiao, 1973; Niu et al., 2014; Rennenberg et al., 2006; Sperlich, Chang, Penuelas, Gracia, & Sabate, 2015). As a result, photosynthesis is reduced. Numerous studies on a variety of tree species found rising C_a to mitigate restrictions on C assimilation under declining water availability due to increased leaf internal CO_2 concentrations (C_i) and suppressed photorespiration (Ainsworth & Rogers, 2007; Birami et al., 2020; Dusenge, Duarte, & Way, 2019; Pushnik et al., 1995). CO_2 enrichment generally triggers decreases in stomatal conductance (g_s) and increases in water-use efficiency (WUE) often going along with reduced transpiration rates (E) (Birami et al., 2020; Dusenge et al., 2019; Haworth, Heath, & McElwain, 2010). As a possible outcome of this, soil water may be preserved, potentially slowing water stress development. However, if a decrease in leaf-level E is accompanied by growth stimulation and hence increases in leaf area, these two [CO_2] effects could most likely counterbalance each other (Jin, Ainsworth, Leakey, & Lobell, 2018; Knauer et al., 2017; Tor-ngern et al., 2015).

While there is some knowledge on elevated [CO_2] (eCO_2) impacts on tree drought responses, little is known about possible effects of elevated CO_2 on stress thresholds and time-to-mortality during a lethal drought (but see Bartlett, Klein, Jansen, Choat, & Sack, 2016 for an in-depth overview of hydraulic drought tolerance thresholds). Duan et al. (2014) suggested that eCO_2 (+240 μl l^{-1}) has no effect on time-to-mortality during drought in either *Pinus radiata* or *Callitris rhomboidea* seedlings and that air temperature is more influential than [CO_2] on drought responses (Duan et al., 2015). However, these studies monitored leaf gas exchange only on a weekly basis. In order to get a more detailed impression on mortality risk and the chronological sequence of events leading to mortality, continuous gas exchange measurements at the whole tree level along with a closely timed monitoring of the hydraulic status could be of particular importance (Hartmann et al., 2018; Ryan, 2011).

In connection with tree mortality, carbon starvation and hydraulic failure have been identified and discussed as the two main processes causing tree death. Carbon starvation is defined to occur when C requirements for respiration exceed C assimilation during stomatal closure (Adams et al., 2010; Hartmann, 2015). Under such conditions, C reserves namely non-structural carbohydrates (NSC) gain enormous importance for osmoregulation and maintaining physiological functioning (Hartmann, 2015). The ability to access and mobilize these reserves has been shown to support tree survival (Mitchell et al., 2013; Sevanto, 2018; Sevanto, Mcdowell, Dickman, Pangle, & Pockman, 2014). As NSCs have been found to increase under eCO_2 (Ainsworth & Long, 2004), trees may benefit from this during drought conditions. Moreover, the longer the drought the more critical are NSC reserves to sustain respiration rates (Mitchell et al., 2013), which might further enhance any potential benefit from eCO_2.

The process of hydraulic failure in drought mortality has been recently identified as the most prominent cause of tree death (Brodribb et al., 2020). It is mainly associated with turgor loss and decreases in xylem conductivity ultimately leading to tissue dehydration (Hsiao, 1973) and xylem embolisms (Brodribb & Cochard, 2009). Values between 50 and 80 % loss in xylem hydraulic conductivity have been related to tree death in conifers (Brodribb & Cochard, 2009; Hammond et al., 2019). Although C starvation and hydraulic failure were at first considered as separate causes (McDowell et al., 2008), such a distinction has proven to be difficult. Carbon and water processes in trees are tightly interconnected as the transport of assimilates for example depends on phloem velocity and NSCs, as osmolytes, are crucial for maintaining turgor pressure (Adams et al., 2017; Duan et al., 2018; Hartmann et al., 2018).

In the attempt to attribute a cause of tree mortality, the identification of general critical thresholds or tipping points beyond that death is inevitable, has been a much sought objective (Brodribb & Cochard, 2009; Hammond & Adams, 2019; O'Brien et al., 2017; Resco et al., 2009). However, defining such tipping points is associated with enormous difficulties as there is no general consensus on when a tree can be declared dead (see Hartmann et al., 2018). This leaves the question whether a specific threshold marks a tree in the process of dying or a tree that is already dead (Hammond et al., 2019). Regardless of this uncertainty, recent studies have suggested drought-related thresholds that may critically impair tree functioning (Bartlett et al., 2016; Ruehr, Grote, Mayr, & Arneth, 2019), including a tree's C balance turning negative, stomatal closure, leaf turgor loss point and substantial loss of xylem conductivity. However, it has yet to be investigated if elevated [CO_2] may affect these thresholds during drought.

While in a previous study we could show that eCO_2 can modestly impact heat and hot-drought stress responses in Aleppo pine seedlings (Birami et al., 2020), we followed here the assumption that tree survival under prolonged drought stress might benefit from greater NSC reserves (e.g., Mitchell et al., 2013), stimulated by eCO_2. Hence, we assessed the time-to-mortality during a fast and a slow lethal drought to identify the importance of NSC for survival. In addition, we assessed if critical physiological drought thresholds and mortality risk of *P. halepensis* seedlings are altered by eCO_2.

In contrast to the majority of previous studies, we designed our elevated [CO_2] treatment according to CO_2 concentrations prescribed for the RCP8.5 at the end of this century (range 794–1,142 ppm) (Collins et al., 2013) and are therefore much higher than in most studies. Although some voices are currently critical of the scenario (Hausfather & Peters, 2020), our treatment design (internal [CO_2] of about 630 ppm) is close to the value given for CO_2-saturated photosynthesis of 600 and 800 ppm for internal [CO_2] (Benner, Sabel, & Wild, 1988; Greer, 2019; Maruyama, Nakamura, Marenco, Vieira, & Sato, 2005; Roberntz & Stockfors, 1998), we should be able to observe a maximum benefit of elevated CO_2 in our study. Hence, our

seedlings were grown either under ambient (*c*. 407 ppm) or highly elevated [CO_2] (*c*. 936 ppm) under controlled conditions for 2 years from seeds originating from the Yatir forest in Israel. The Yatir forest is dominated by *P. halepensis* and has been planted *c*. 1965 at the northern edge of the Negev desert (Grunzweig, Lin, Rotenberg, Schwartz, & Yakir, 2003).

As current climate conditions in the Yatir forest are already highly stressful and contrasting with natural sites of *P. halepensis* in Israel, the question is under consideration whether the forest is particularly at risk under predicted climate change. In light of this, our hypotheses were: (a) larger net C uptake and enhanced water-use-efficiency as long-term acclimation to highly elevated [CO_2] benefit the survival of *P. halepensis* seedlings during drought, (b) the [CO_2] advantage is more pronounced during a slow lethal drought compared with a fast lethal drought as NSC reserves are more crucial when carbon starvation becomes the main mortality risk, and (c) the [CO_2] benefit is apparent in the change of critical thresholds of mortality risk factors resulting in the prolonging of the time-to-mortality in *P. halepensis* seedlings.

2 | MATERIAL AND METHODS

2.1 | Plant material

Pinus halepensis (Miller) seedlings—seeds originating from trees in the vicinity of the flux tower in the Yatir forest, Israel (31°20′49.2″N, 35°3′7.2″E)—were grown either under ambient (407 ± 23 ppm) or elevated (936 ± 9 ppm) [CO_2] (Supplement 1b) in a greenhouse facility in Garmisch-Partenkirchen, Germany (732 m a.s.l., 47°28′32.87″N, 11°3′44.03″E). The seedlings were cultivated for 24 months and repotted twice in a mixture of C-free potting substrate. After germination in vermiculite, seedlings were transferred to 0.25-L pots containing a C-free potting substrate (1:1:0.5 quartz sand (0.7 mm and 1–2 mm), vermiculite (*c*. 3 mm) and quartz sand (Dorsolit 4–6 mm) and expanded clay (8–16 mm)) enriched with 2 g of slow-release fertilizer (Osmocote® Exact + TE 3–4 month fertilizer 16–9–12 + 2MgO + TE, ICL Specialty Fertilizers, Geldermalsen, The Netherlands) and liquid fertilizer (Manna® Wuxal Super, Wilhelm Haug Gmbh & Co. KG, Ammerbuch, Germany), and were finally placed into 4.5-L pots holding substrate (1:1:2 vermiculite (3–6 mm), coarse (4–6 mm) and fine quartz sand (2–3 mm) with expanded clay (8–16 mm)) enriched with 5 g of slow-release fertilizer (Osmocote® Exact Standard 5-6 M fertilizer 15–9-12 + 2MgO + TE, ICL Specialty Fertilizers, Geldermalsen, The Netherlands), liquid fertilizer and phosphate-magnesium addition once. Throughout, environmental conditions were maintained constant between the two treatments (ambient [CO_2] (aCO_2) and elevated [CO_2] (eCO_2)) with no significant differences in daily air temperatures (T_{Air}) (daytime: 21.5 ± 2.9 °C, nighttime: 15.5 ± 2.1 °C, CS215, Campbell Scientific, Logan, UT), relative humidity (RH, 74.6 ± 15.7 %) (Supplement 1c), relative soil water content (RWC, watered to full saturation) and photosynthetic active radiation (PAR) (on average 662 ± 286 μmol m^{-2} s^{-1}, PQS 1, Kipp & Zonen, Delft, The Netherlands) (Supplement 1d). During the winter month (December to February), seedlings were kept at reduced T_{Air} and RWC, which afterwards was reversed to previous control conditions (Supplement 1a,e). Additionally, seedlings were subjected to a drought period of approximately 30 days with RWC of <20 % 9 months prior to the main experiment to mimic natural summer drought conditions in the Yatir forest (Preisler et al., 2019). The placement of the CO_2 treatments within the two greenhouse compartments was iterated in 1–2 monthly intervals.

2.2 | Experimental setup

In order to monitor gas exchange throughout the lethal drought experiment, nine seedlings per CO_2 treatment were randomly selected and each of these seedlings was placed into its own tree chamber within the greenhouse to measure above- and belowground gas exchange separately (Birami et al., 2020) (Supplement 2). The tree chambers consisted of a light transmitting aboveground compartment separated gas tight from the opaque belowground compartment. Chambers were constantly supplied with an air stream of pre-defined [H_2O] and [CO_2] depending on the respective treatment (aCO_2: 413.67 ± 57.49 ppm; eCO_2: 914.36 ± 31.35 ppm).

Conditions in the tree chambers were kept at day-time mean T_{Air} (5SC-TTTI-36-2 M, Newport Electronics GmbH, Deckenpfronn, Germany) of 24 °C (Figure 1a) (night temperatures of about 20 °C) and PAR (PQS 1, Kipp & Zonen, Delft, the Netherlands) was on average 476 μmol m^{-2} s^{-1} for 16 hr during daytime (Figure 1f) by supplementing outside light with plant growth lamps (T-agro 400 W; Philips, Hamburg, Germany). Lower levels of PAR are not untypical at the forest floor and we found that our seedlings reached 77 % (aCO_2)/67 % (eCO_2) of their maximum photosynthesis as derived from light response curves at a PAR of 500 μmol m^{-2} s^{-1} (Supplement 3). Since we omitted from increasing the supply of water vapor to the aboveground tree chambers during drought progression, vapor pressure deficit (VPD) increased similar to observations at the Yatir site (Tatarinov et al., 2016). Hence, decreasing transpiration rates (*E*) gradually decreased RH from 50 % to 20 % with increasing soil drought (Figure 1d). Accordingly, VPD increased from 1–2 kPa to values near 3 kPa (Figure 1c). Since soil temperature (T_{Soil}) (T107, Campbell Scientific Inc., Logan, UT) was not actively controlled, temperatures ranged between 20 and 27 °C but were similar in all chambers (Figure 1b).

RWC (10HS, Decagon Devices, Inc., Pullman, WA) under control conditions was maintained at about 50 % (Figure 1e). Before stopping irrigation completely, water availability was progressively reduced in five steps simulating a slow lethal drought (Table 1). Slightly higher RWC under eCO_2 resulted from lower *E*, which also explains higher $\%_{Emax}$ values.

With the experimental setup just described and also nine Aleppo pine seedlings per [CO_2] treatment (not the same seedlings as in the slow drought experiment) we previously conducted an experiment mimicking a fast, lethal drought by only reducing irrigation twice before stopping it all together after 2 weeks. Air temperature and

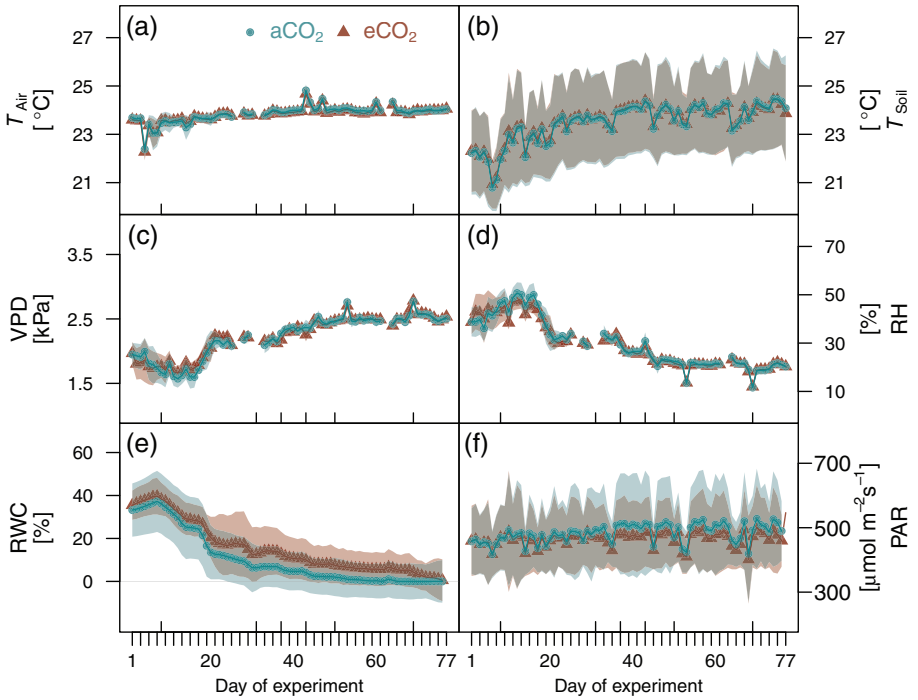


FIGURE 1 Environmental drivers during the lethal drought in the aCO_2 (*c*. 413 ppm) and eCO_2 (*c*. 914 ppm) treatment. Air temperature (T_{Air}, a), soil temperature (T_{Soil}, b), vapor pressure deficit (VPD, c), relative humidity (RH, d), relative soil water content (RWC, e) and photosynthetic active radiation (PAR, f) are shown. Lines and symbols mark daily treatment averages during daytime (PAR >100) and the shaded areas are ±*SD* (*n* = 9)

TABLE 1 Irrigation modulation during the seven experimental steps (I–VII) of the lethal drought simulation in relation to the pre-determined maximum of transpiration per treatment

Step		I	II	III	IV	V	VI	VII
Days		7	21	8	6	7	19	9
Irrigation [ml day^{-1}]		300	100	50	37.5	30	16.7	0
Irrigation $\%_{Emax}$	aCO_2	500	83	42	31	21	14	0
	eCO_2	582	97	49	36	24	16	0

Note: Shown are length of each irrigation step in days and irrigation amount in ml per day as well as in % of the maximum water loss through transpiration ($\%_{Emax}$).

relative humidity of the tree chambers and the initial RWC did not differ between the two experiments (Supplement 4).

2.3 | Gas exchange measurements

Above- and belowground CO_2 and H_2O gas exchange (*n* = 9 per [CO_2] treatment) was quantified using two gas analysers connected in series. First, absolute [CO_2] and [H_2O] of the supply air stream (LI-840, Li-cor, Lincoln, NE) and secondly, differences between supply and sample air stream (Li-7,000, Li-cor, Lincoln, NE) were measured. While automatically switching between chambers every 120 s, the data was logged to a computer at 10 s intervals. CO_2 fluxes from the belowground compartment were treated as root respiration signal because all belowground C was planted related as C-free substrate has been used as potting material (see above). Two empty chambers containing the same C-free potting substrate, but without seedlings, were used as blanks to constantly monitor the system and to correct gas exchange estimates for any fluctuations in [CO_2] and [H_2O] not caused by changes in plant activity (3.09 ± 2.36 ppm CO_2 and −0.05 ± 0.05 ppt H_2O in the above- and 4.74 ± 2.77 ppm CO_2 in the belowground compartment). For each chamber measurement, only the last 40 s were used to calculate gas exchange fluxes according to the following equations.

Tree transpiration rate (*E*) in [mol s^{-1}] was calculated as

$$E = \frac{F_m\left(W_{supply} - W_{sample}\right)}{\left(1 - W_{sample}\right)}, \quad (1)$$

with W_{supply} [mol mol^{-1}] as [H_2O] in supply air stream, W_{sample} [mol mol^{-1}] as [H_2O] in sample air stream and F_m [mol s^{-1}] as molar flow.

Tree net assimilation ($A_{net,\ canopy}$) as well as root and night-time shoot respiration in [mol s^{-1}] were calculated using the equation for CO_2 fluxes

$$CO_2\ \text{flux} = -F_m\left(C_{supply} - C_{sample}\right) - EC_{sample}, \quad (2)$$

with C_{supply} [mol mol^{-1}] as [CO_2] in supply air stream, C_{sample} [mol mol^{-1}] as [CO_2] in sample air stream, F_m [mol s^{-1}] as molar flow

and E [mol s^{-1}]. Total daily respiration rates (R_{total}) were then calculated from the sum of nighttime shoot and day-and nighttime root respiration.

Canopy conductance (g_{canopy}) was determined from daytime gas exchange data as follows

$$g_{canopy} = \frac{E\left(1000 - \frac{W_{leaf} + W_{sample}}{2}\right)}{W_{leaf} - W_{sample}}, \quad (3)$$

with W_{leaf} as leaf saturated vapor pressure, W_{sample} [mol mol^{-1}] as [H_2O] in sample air stream and E [mol s^{-1}]. This approach neglects boundary layer conductance, which should be negligible under high mixing conditions inside the chamber (Birami et al., 2020).

Leaf internal CO_2 concentration (C_i) [μmol mol^{-1}] was calculated using the following equation

$$C_i = \frac{\left(\frac{g_{canopy}}{1.6} - \frac{E}{2}\right)C_{sample} - A_{net\ canopy}}{\frac{g_{canopy}}{1.6} + \frac{E}{2}}, \quad (4)$$

with C_{sample} [μmol s^{-1}] as [CO_2] in sample air stream, g_{canopy} [mol s^{-1}] as canopy conductance, $A_{net\ canopy}$ [μmol s^{-1}] as net assimilation and E [mol s^{-1}].

2.4 | Sampling procedure and needle water status

Throughout the experiment we sampled needle material for non-structural carbohydrates analysis and tree water status. The sampling was conducted between 12 p.m. and 2 p.m. Midday needle water potential (Ψ_{md}) was measured using a pressure bomb (Model 1000, PMS Instrument Company, Albany, OR) on one needle fascicle per tree. Additionally, in order to determine relative needle water content (RLWC) needle mass was determined (a) from the same fresh needles used for water potential analysis, (b) after being submerged in distilled water for 48 hr and (c) post drying at 60 °C. We defined a sudden sharp drop in RLWC and Ψ_{md} as indication that the turgor loss point has been reached. Needle samples for non-structural carbohydrate analysis were immediately frozen in liquid nitrogen and stored at −80 °C until further analysis. Tree biomass was harvested at the last day of the experiment when seedlings appeared dead and divided into needle, woody and root tissue and dried at 60 °C for 48 hr prior dry mass was measured.

2.5 | Non-structural carbohydrate quantification

2.5.1 | Soluble sugar

The determination of soluble sugar was conducted as described by Landhäusser et al. (2018) with minor modifications. For the extraction, 15 mg of frozen plant powder was added to 0.5 ml 80 % ethanol. After shaking, 10 min incubation at 80 °C and centrifugation (13,000*g* for 3 min), the supernatant was taken and the extraction process repeated twice. While the remaining pellet swelled in 1 ml distilled water (dH_2O) at 95 °C for 2 hr before being stored at −80 °C for subsequent starch analysis (see below), the supernatants were mixed and the fluids were vaporized in a vacuum concentrator. The pellet was then dissolved in 1 ml dH_2O. For sugar quantification, 200 μl aliquots of extract (1:10 diluted in dH_2O) were mixed with 100 μl invertase solution (300 U ml^{-1} (Sigma-Aldrich I4504-250 mg, Merck, Darmstadt, Germany) diluted in 10 mM sodium acetate buffer (pH 4.5) and incubated for 35 min at 55 °C). Afterwards 200 μl (5 mM MgCl, 95 mM Tris–HCl, 1.7 mM ATP, 4.5 mM NAD+, 1.1 U ml^{-1} G6PDH (Sigma-Aldrich G8404-2KU, Merck, Darmstadt, Germany), 10 U ml^{-1} HK (Roche 1,142,632,001), 1.6 U ml^{-1} phosphoglucose isomerase (Sigma-Aldrich P5381-1KU, Merck, Darmstadt, Germany)) were added to 50 μl aliquots of sugar extract in 96-well microtest plates (Brand, Wertheim, Baden-Württemberg, Germany). After 20 min of incubation at room temperature, absorbance was determined at 340 nm with a microplate absorbance reader (Epoch2, BioTek, Winooski, VT).

2.5.2 | Starch

After thawing and shaking, 80 μl aliquots of water diluted starch samples (see above) were mixed with 20 μl α-amylase (30 U ml^{-1}, Megazyme E-BLAAM-10 ml) and boiled at 85 °C for 1 hr. Following a quick cooling, 100 μl amyloglucosidase (20 U ml^{-1} amyloglucosidase (Sigma-Aldrich 10,115-1G-F, Merck, Darmstadt, Germany) dissolved in 25 mM potassium acetate buffer) were added and samples boiled at 55 °C for another hour. In preparation for the analysis, samples were cooled again and centrifuged (13,000*g* for 3 min) before 50 μl aliquots were mixed with 200 μl buffer (5 mM MgCl, 95 mM Tris–HCl, 1.7 mM ATP, 4.5 mM NAD+, 1.1 U ml^{-1} G6PDH (Sigma-Aldrich G8404-2KU, Merck, Darmstadt, Germany), 10 U ml^{-1} HK (Roche 1,142,632,001, Roche, Mannheim, Germany), 10 U ml^{-1} HK) in 96-well microtest plates (Brand, Wertheim, Baden-Württemberg, Germany). Absorbance at 340 nm was measured using a microplate absorbance reader (Epoch2, BioTek, Winooski, VT).

2.6 | Statistical data analyses

Gas exchange data of each chamber were quality controlled. Day and nighttime measurements outside 1.5 times the interquartile range above the upper quartile or below the lower quartile, which were adjusted for each experimental phase, were considered outliers and therefore not included in the analysis. This removed on average 5.2 and 8.4 % of the CO_2 and H_2O gas exchange data, respectively.

All statistical analyses were performed using R 3.5.2 (R Core Team 2016). Differences were considered significant at $p \leq .05$. Treatment and drought effects were assessed by fitting linear mixed effects models (lme) (package lme4: Bates, Maechler, Bolker, & Walker, 2015 and package lmerTest: Kuznetsova, Brockhoff, & Christensen, 2017) with time and treatment as fixed effects and tree as random factor.

Additionally, *post-hoc* Tukey multiple comparisons test of means (package emmeans: Lenth, 2019) was performed to assess daily differences. Differences in biomass were tested using *t*-test for two independent samples. The correlation between needle soluble sugar (SS_N) to starch (St_N) ratios and needle water potential Ψ_{md} was fitted using a Michaelis–Menten kinetics function ($y = ax[b + x] - 1$). A logarithmic function ($y = \log[x]$) was used to simulate the tree C balance response to stomatal closure.

To assess possible [CO_2] effects on tree mortality risk factors during the lethal drought we first identified core parameters associated with tree survival such as tree C balance, stomatal closure and hydraulic integrity. We then defined critical thresholds for these parameters (see Section 3) and determined the probability for seedlings to match these threshold criteria per day. Aiming to assess the tree mortality risk, we combined the separate parameter observations by quantifying the probability for seedlings to reach all three critical thresholds per day. All these evaluations were made for aCO_2 and eCO_2 separately. We used logistic regression to analyse the [CO_2] effect on risk threshold probability per day, and accounted for temporal autocorrelation by bootstrap sampling. We assessed model performance using a pseudo R^2 metric (package sigr, Mount & Zumel, 2019). Significant differences between treatments were assessed via a non-parametric Mann–Whitney-U-Test comparing the average number of days required to reach the threshold per treatment.

As indicators of tree death, we used foliar browning, cessation of shoot respiration and midday leaf water potential (Ψ_{md}) below −5 MPa, which is associated with 50% potential loss of xylem conductivity (PLC50) in *P. halepensis*.

3 | RESULTS

3.1 | [CO_2] effect under favorable conditions

Atmospheric [CO_2] had a clear effect on the biomass of Aleppo pine seedlings resulting in significantly higher shoot and root biomass under eCO_2 (needle +27 %; woody tissue +30 %; root +27 %) (Table 2). However, root/shoot ratios were similar to aCO_2.

TABLE 2 Biomass (*P. halepensis*, $n = 9$ per treatment, ±*SD*) of needles, shoot woody tissue, roots and shoot/root ratio was measured at tree death

	aCO_2 (*c.* 413 ppm)			
Tissue	**Biomass [gDW]**		**eCO_2 (*c.* 914 ppm)**	
Needle	41.38 ± 8.88	(a)	52.56 ± 6.15	(b)
Woody tissue	26.96 ± 5.81	(a)	34.97 ± 5.03	(b)
Root	80.72 ± 12.57	(a)	102.59 ± 13.28	(b)
Root/shoot	1.11 ± 0.21		1.16 ± 0.21	

Note: Using *t*-test for two independent samples tested for potential treatment effects. Statistical significance (*t*-test, $p < .05$) is indicated by different lower case letters.

During 12 days of acclimation to the tree chambers under sufficient water supply, tree transpiration (*E*) and canopy net photosynthetic rates ($A_{net,\ canopy}$) steadily increased. $A_{net,\ canopy}$ rates were twice as high in eCO_2 than in aCO_2 (Tukey HSD: $p = .014$, $t = -5.15$) on the tree level reaching maximum rates of 1.24 ± 0.17 (aCO_2)/1.98 ± 0.71 (eCO_2) [mol hr^{-1} $tree^{-1}$] (Figure 2b). Simultaneously, tree *E* was not significantly lower in eCO_2 than aCO_2 (Figure 2a) on the tree level, reaching maximum rates of 0.40 ± 0.06 (aCO_2)/0.31 ± 0.11 (eCO_2) [mol hr^{-1} $tree^{-1}$]. On a leaf area basis, the [CO_2] effect on $A_{net,\ canopy}$ vanished suggesting the increase in leaf area as the main reason for higher $A_{net,\ canopy}$ in eCO_2 (Supplement 5b). In contrast, treatment differences in *E* were significantly amplified on a leaf area basis (Tukey HSD: $p = .021$, $t = 5.113$) (Supplement 5a), which can be explained by lower canopy conductance (g_{canopy}, sum of stomatal and cuticular conductance) in eCO_2 of 22 % at the tree level and 33 % at the leaf level (leaf areadata not shown). Respiration rates [sum of shoot nighttime, root day- and night-time respiration (R_{total})] were not significantly higher under eCO_2 compared to aCO_2, despite a significantly larger tree biomass (+27 %) under eCO_2.

3.2 | Gas exchange response to drought

In the course of step-wise reductions in irrigation, *E* and $A_{net,\ canopy}$ declined gradually and reached new stable rates during each drought phase. Simultaneously, treatment differences in $A_{net,\ canopy}$ and *E* diminished with progressing drought. In contrast, the [CO_2] effect on R_{total} apparent in 1.5 times higher rates in eCO_2 compared to aCO_2 (not statistically significant) was largely sustained by concurrently decreasing R_{total} in both treatments with increasing soil drought (Figure 2d). Interestingly, ceasing irrigation completely triggered a sudden respiration burst notable in $A_{net,\ canopy}$ as well as R_{total} (Figure 2c,e). Contrary to the transition from assimilation to respiration in $A_{net,\ canopy}$, the renewed rise in R_{total} was significant (Tukey HSD: aCO_2 $p < .01$, $t = 6.99$; eCO_2 $p < .01$, $t = 9.72$) due to a doubling of respiration rates during the burst. This phenomenon had also been observed during the prior, fast lethal drought experiment (Supplement 4a,c). Since occurring at times when trees started dying, the burst in respiration may indicate drought-induced lethal cell damage.

3.3 | [CO_2] effect on tree C balance during drought

We further assessed the [CO_2] effects on the tree C balance ($\Sigma C = A_{net,\ canopy} - R_{total}$, see also Supplement 6b) and water loss (ΣE, see also Supplement 6a) in relation to g_{canopy}. To overcome the differences in g_{canopy} from [CO_2], g_{canopy} was expressed in relation to maximum g_{canopy} ($g_{canopy\ max}$) per treatment (Figure 3). Based on changes in C_i/C_a ratios, which remained unaffected by [CO_2], we have separated drought effects on assimilation into four phases (see Figure 3, dashed vertical lines). Following this structuring, we analysed the [CO_2] effect on ΣC in the course of declining g_{canopy}.

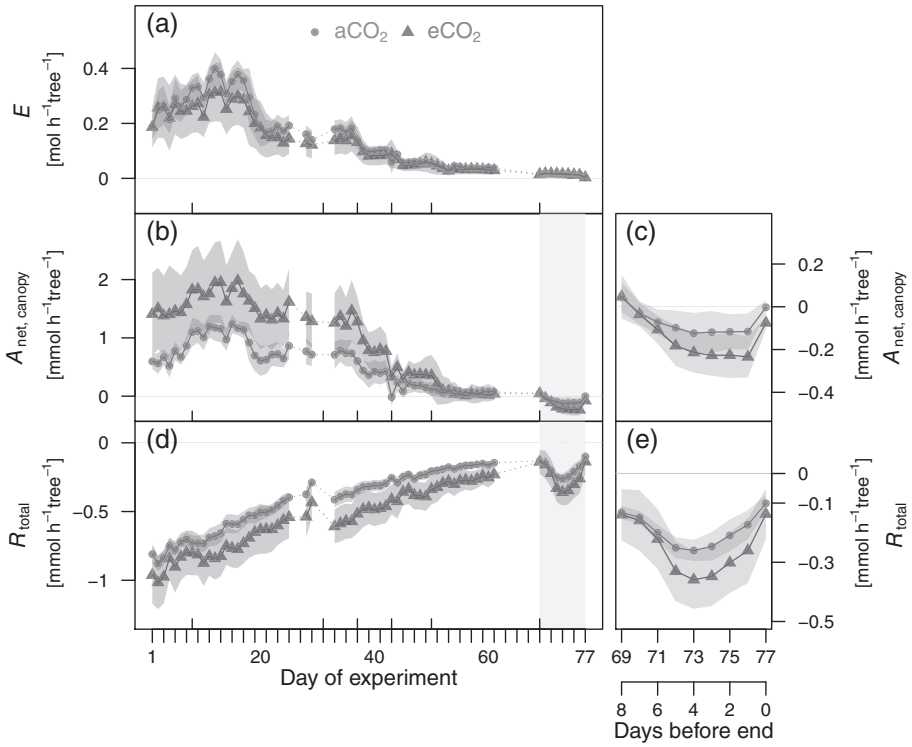


FIGURE 2 Gas exchange parameters during the course of the lethal drought experiment. Shown are transpiration (*E*) (a), net assimilation ($A_{net\ canopy}$) (b) and respiration (R_{total}, sum of shoot dark and root respiration) (d) rates as hourly treatment (aCO_2:*c*. 413 ppm, eCO_2:*c*. 914 ppm) means per day and tree. The shaded areas depict ±*SD*. Data gaps are bridged by thin dotted lines. For$A_{net\ canopy}$andR_{total}, the light grey colored areas mark the final phase of the experiment, which is additionally shown on a finer scale (c, e) highlighting the respiration burst just before death of the seedlings occurred. Longer tick marks on thex-axis mark days of irrigation reductions [Colour figure can be viewed at wileyonlinelibrary.com]

During non-stressful conditions, indicated by C_i/C_a ratios of about 0.7 (phase I), assimilation was not limited by water availability (irrigation step one and the beginning of step two) and ΣC in eCO_2 was with 0.17 g C day^{-1} about 300 % higher than in aCO_2 (Tukey HSD: p = .012, t = –4.90). With developing drought stress (during irrigation steps two and three), as stomatal restriction on assimilation increased causing C_i/C_a ratios to decline (at 40–60 %$g_{canopy\ max}$), the stimulation of eCO_2 on ΣC also declined. In phase III, when C_i/C_a is nearly stagnant again at about 0.6 (at around 35 % $g_{canopy\ max}$), the restriction on assimilation is slowly transitioning from stomatal to non-stomatal accompanied by again increasing relative difference in ΣC between aCO_2 and eCO_2. However, high variances of drought stress development within the treatments prevented these differences from being statistically significant. Sharply increasing C_i/C_a ratios mark the reaching of the C_i inflexion point and simultaneously the beginning of phase IV. During this last phase (irrigation steps 4–7) characterized by dominating and further increasing non-stomatal restrictions on assimilation, the $[CO_2]$ effect transitioned from a benefit to a detriment at 15 % of $g_{canopy\ max}$ (Ψ_{md} of −2.3 MPa). This goes along with the transition from assimilation to respiration during the last week of the experiment (C_i/C_a > 1) and higher respiration rates in eCO_2 (Figure 2b,c). In contrast to the $[CO_2]$ effect on ΣC, the difference in ΣE between treatments (on average – 12 ± 5 %) was not significant at the tree level, as variances were high and the larger biomass under eCO_2 almost annulled the effect of reduced *E* per unit leaf area.

3.4 | Needle water potential and non-structural carbohydrates

Despite treatment differences in tree water fluxes (g_{canopy}, *E*) on the leaf level, midday leaf water potential (Ψ_{md}) and relative leaf water content (RLWC) measurements revealed no $[CO_2]$ effect (Figure 4). Following a slow but steady decrease during mild to moderate drought stress, Ψ_{md} fluctuated around the turgor loss point identified at −2.2 MPa as water availability was further reduced (Table 1, 16.7 ml day^{-1}). While the decline in Ψ_{md} responded to increasing drought, RLWC was maintained at values between 70 and 80 %. However, once the turgor loss point was reached, Ψ_{md} and RLWC steeply declined reaching values of about −7 MPa and 31 ± 16 %, respectively, within 8 days after irrigation had been stopped.

Similar to Ψ_{md}, needle soluble sugar (SS_N) content was not affected by elevated $[CO_2]$ (Figure 4a). In addition, SS_N showed no drought effect, as concentrations were maintained relatively stable. The observed slight decrease in SS_N at the final harvest could be due to metabolic processes triggered by tree death (Figure 4a). As a consequence of these SS_N results, steadily rising SS_N to needle starch (St_N) ratios (Figure 5) were mainly attributed to decreasing St_N concentrations (Figure 4b). In the course of the experiment, St_N reserves were depleted by about 80 and 85 % in aCO_2 and eCO_2, respectively. Accordingly, the distinct $[CO_2]$ effect on SS_N/St_N ratios under mild and moderate drought (Ψ_{md} > −2.2 MPa) resulted from St_N concentrations being twice as high in eCO_2 than in aCO_2 (Tukey HSD: p < .001, t = –6.27). However, this treatment effect diminished with amplifying drought due to stronger decreasing St_N concentrations in eCO_2 compared to aCO_2, while the overall St_N concentration remained higher under eCO_2. The course of SS_N/St_N ratios indicates the use of St_N to maintain SS_N levels and respiration during drought. Furthermore, it would explain the increased reduction of St_N in eCO_2, as assimilation per leaf dry weight in eCO_2 was lower than in aCO_2 after reaching the turgor loss point. Similar developments of SS_N/St_N ratios in relation to Ψ_{md} could be observed during a prior fast lethal drought experiment (Figure 5, Supplement 4).

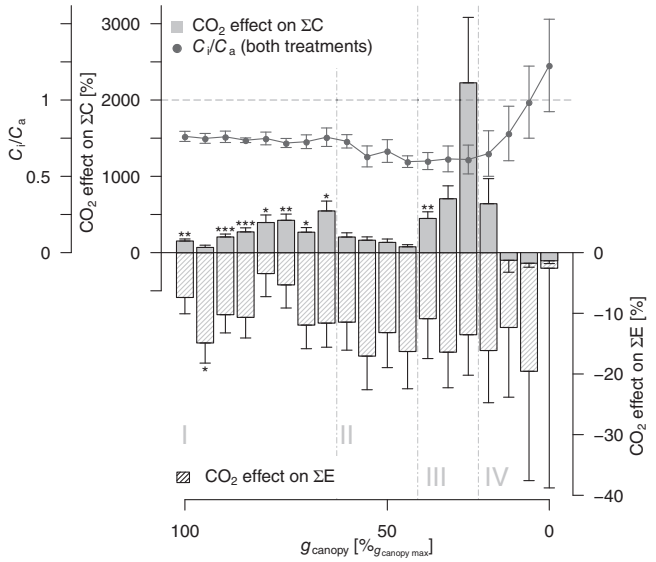


FIGURE 3 [CO_2] effect on tree carbon balance (ΣC) and tree water loss from transpiration (ΣE) as well as C_i/C_a ratios (for day-time measurements, PAR > 100 μmol m^{-2} s^{-1}) over the course of stomatal closure. ΣC (sum of net assimilation, shoot dark and root respiration, grey bars) and ΣE (sum of shoot day and night transpiration, shaded bars) are shown as treatment differences in percentage of aCO_2 values (%-treatment = ([eCO_2 − aCO_2]/aCO_2) × 100). The degree of stomatal closure was calculated by expressing canopy conductance (g_{canopy}, sum of stomatal and cuticular conductance) as percentage of maximum g_{canopy} under control conditions for each treatment. Bars show averages over 5 % bins of g_{canopy} expressed as percentage of maximum g_{canopy} with error bars depicting SD. C_i/C_a values are also shown as means over 5 % bins of g_{canopy} ± *SD* for both treatments. Asterisks above bars represent statistical significance (linear mixed effects model with *post-hoc* Tukey; p < .05*, p < .01**, p < .001***) of the [CO_2] effect derived from absolute values. Grey dashed lines and roman numerals mark the four phases of assimilation restriction differentiated by changes in C_i/C_a ratios in the course of declining g_{canopy} [Colour figure can be viewed at wileyonlinelibrary.com]

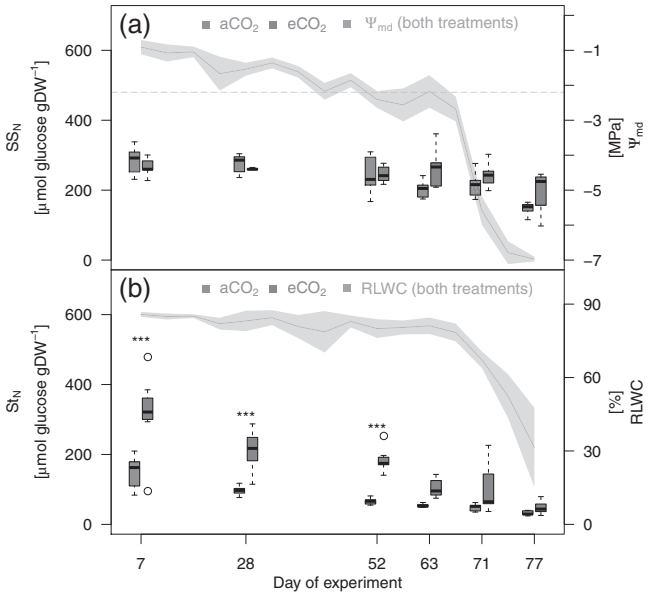


FIGURE 4 Needle soluble sugar (SS_N, a), needle starch (St_N, b) concentrations, midday needle water potential (Ψ_{md}, a) and relative needle water content (RLWC, b) over the course of the experiment. Ψ_{md} and RLWC are shown as average over both treatments ±*SD* depicted as shaded area. The turgor loss point at −2.2 MPa is marked as grey dashed line. SS_N and St_N are shown as boxplots with measurements outside 1.5 times the interquartile range above the upper quartile or below the lower quartile considered outliers. Asterisks above boxes represent statistical significance between treatments (linear mixed effects model with *post-hoc* Tukey; p < .05*, p < .01**, p < .001***) [Colour figure can be viewed at wileyonlinelibrary.com]

3.5 | [CO_2] effect on risk thresholds during lethal drought

We used critical values to assess differences in the probabilities of reaching critical thresholds between the CO_2 treatments (see 'Statistical data analysis'). The threshold criteria we assigned were: negative ΣC, daytime g_{canopy} ≤ 5 % $g_{canopy\ max}$ and Ψ_{md} below the turgor loss point (−2.2 MPa). We preferred turgor loss to PLC50, as we did not directly assess PLC50 in our seedlings. To test if eCO_2 might affect drought-induced carbon starvation, we introduced a 50 % threshold for St_N (relative to the initial values) (NSC_{50}), although there is no consensus on critical NSC values (Adams et al., 2017).

The treatment difference was only significant in St_N (Figure 6d); here aCO_2 seedlings reached the NSC_{50} threshold earlier and faster (Mann–Whitney-U-Test: p = .019). Furthermore, declines in St_N followed shortly after ΣC turned negative in aCO_2 (Figure 6a), whereas a time lag of about 10 days between these two events was observed in eCO_2 suggesting a positive [CO_2] effect on the carbon safety margin. While for ΣC (Figure 6a) and Ψ_{md} (Figure 6c) the probability of reaching the respective threshold increased slowly, the transition in g_{canopy} (Figure 6b) indicating stomatal closure was rather sudden, changing the probability from zero to one within 2 days irrespective of [CO_2]. Interestingly, these 2 days were the same in both treatments indicating that the relative response of g_{canopy} to severe drought was identical in aCO_2 and eCO_2.

When we assessed the overall risk factor by combining the results for ΣC, Ψ_{md} and g_{canopy} (Figure 6e), it became apparent that [CO_2] did not affect the probability of reaching the threshold, nor the timing of mortality. Ψ_{md} declining below the turgor loss point clearly marked the time at which survival in both treatments became critical. In summary, this clearly indicates that the mortality risk under severe drought stress was not reduced by elevated [CO_2]. Furthermore, our results show that this applies to both fast and slow (data not shown) lethal droughts.

4 | DISCUSSION

4.1 | Pre-drought [CO_2] effect

We found eCO_2 to stimulate plant growth, equally reflected in increasing root and shoot biomass and therefore not affecting root/

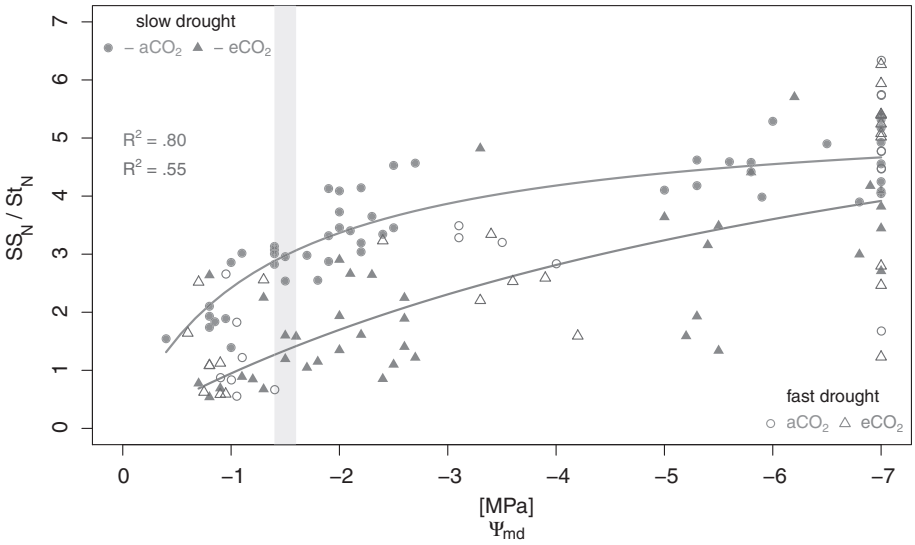


FIGURE 5 Needle soluble sugar (SS_N) to starch (St_N) ratios over midday needle water potential (Ψ_{md}). The turgor loss point at −2.2 MPa is marked as grey dashed line. $SS_N$to St_Nratios are shown as individual measurements for the 2018 slow drought (aCO_2solid points, eCO_2solid triangles) and for the 2017 fast drought (aCO_2points, eCO_2triangles). Lines (aCO_2turquoise, eCO_2dark red) show regressions using non-linear least squares [Colour figure can be viewed at wileyonlinelibrary.com]

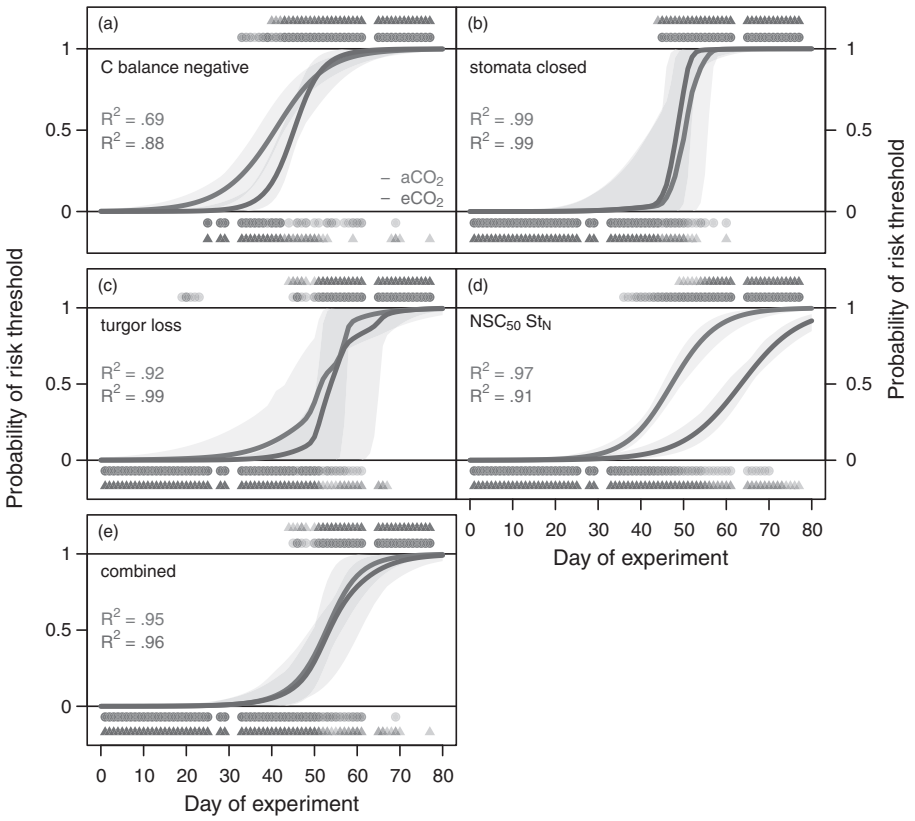


FIGURE 6 Logistic regressions to determine the $[CO_2]$ effect on risk thresholds of Aleppo pine seedlings during a lethal drought (n = 9 per treatment). For carbon balance (a), canopy conductance (g_{canopy}) (b), point of leaf turgor loss (c) and needle starch concentration (St_N) (d). In panel (e) mortality risk for each treatment and day is computed as the combined probability for a tree to present values above risk thresholds for carbon balance, canopy conductance and leaf turgor loss. The critical values were defined as C balance turning negative,g_{canopy}declining below minimumg_{canopy}, Ψ_{md}falling under the turgor loss point (Ψ_{md} < −2.2 MPa) and a 50% loss of St_N(NSC_{50}). The quality of the fitted logistic regressions is shown by 95% confidence intervals depicted as shaded areas and pseudo-R^2values are given. Additionally, the transition of seedlings from 'not meeting the critical threshold' to 'meeting the critical threshold' is shown below and above each regression plot, respectively, with coloring becoming more transparent as number of seedlings decrease [Colour figure can be viewed at wileyonlinelibrary.com]

shoot ratios of the *P. halepensis* seedlings in our study (Table 2). In addition, larger needle starch storage and net C uptake at eCO_2 suggests that excess C was stored as starch in leaves (Eguchi et al., 2004; Poorter et al., 1997; Pritchard, Rogers, Prior, & Peterson, 1999) (Figure 4b). Frequently, increases in $A_{net,\ canopy}$ are accompanied by decreasing E and g_{canopy} under eCO_2 (Ainsworth & Rogers, 2007; Birami et al., 2020; Gamage et al., 2018), as was the case at the leaf level in our study (Supplement 5). An optimization of the stomatal density to stomatal index (stomata to epidermal cells ratio) ratio would account for such an enhanced water-use-efficiency (WUE) (Haworth et al., 2010). However, we did not find a significant $[CO_2]$ effect on stomatal density (p > .1, n = 17) (data not shown). The lack of changes in SD and SI supports the hypothesis that trees more likely respond to eCO_2 by adjusting needle function, which is most prominently done by controlling stomatal aperture (Apple et al., 2000; Bettarini, Vaccari, & Miglietta, 1998; Pritchard et al., 1999). As has been documented in several studies, eCO_2 stimulates stomatal closure (Ainsworth & Rogers, 2007; Birami et al., 2020; Gamage et al., 2018; Xu, Jiang, Jia, & Zhou, 2016). This together with biochemical adjustments most likely resulted in constant ratios of intercellular to

atmospheric [CO_2] (C_i/C_a) in *P. halepensis* leaves under eCO_2 (Figure 3), which is concordant with a previous study (Birami et al., 2020) and suggested scenarios regarding WUE and rising C_a (Lavergne et al., 2019; Saurer, Siegwolf, & Schweingruber, 2004). As a possible underlying mechanism, Tor-ngern et al. (2015) introduced the idea of long-term reductions in E and g_{canopy} being rather indirect, than direct effects of eCO_2. After extensive experiments in a temperate forest (FACE, +200 μmol mol^{-1} for 17 years), they concluded that reductions of g_{canopy} were not a direct stomatal response to increasing [CO_2], but were considered to be attributable to decreases in leaf hydraulic capacity as well as reductions of hydraulic conductance from the xylem to the stomata as long-term acclimation to eCO_2 (Domec et al., 2009; Domec, Palmroth, & Oren, 2016). As our seedlings were grown from seeds under eCO_2 for 2-years such a CO_2 acclimation response might be a likely scenario.

4.2 | [CO_2] effect under mild to moderate drought conditions

Initial responses to drought are typically characterized by a gradual closure of stomata (Blackman et al., 2016; Mackay et al., 2015; Taïbi et al., 2017). During this phase, *P. halepensis* seedlings seemed to be able to offset restrictions on C assimilation under eCO_2 as $A_{net,\ canopy}$ was maintained at higher rates in spite of lower g_{canopy} compared to aCO_2 (Table 2), in agreement to previous observations (Birami et al., 2020). This indicates a potential ameliorating effect of eCO_2 (Ainsworth & Rogers, 2007; Je et al., 2018; Robredo, Pérez-López, Lacuesta, Mena-Petite, & Muñoz-Rueda, 2010), supported by a delay in the C_i inflexion point, which marks the transition from stomatal to non-stomatal limitation as dominant restriction on $A_{net,\ canopy}$ (Flexas, 2002). In our study we did not observed such an effect on the C_i inflexion point as C_i/C_a ratios in *P. halepensis* seedlings were unaffected by [CO_2].

One consideration in connection with reduced g_{canopy} resulting in lower E on the leaf level was a possible preservation of soil moisture and a resulting slowing down of the development of drought stress under elevated [CO_2]. However, such a phenomenon of 'water saving' is debatable due to the trade-off between the reduced water loss through transpiration and the simultaneous increase of leaf area under eCO_2 (Dusenge et al., 2019; Tor-ngern et al., 2015; Wullschleger, Tschaplinski, & Norby, 2002), which was also apparent in our study. In addition, we observed no significant eCO_2 effect on Ψ_{md} or relative leaf water content (RLWC) since *P. halepensis* seedlings in both treatments maintained Ψ_{md} above the turgor loss point (TLP) (−2.2 MPa) and RLWC at around 82% for the longer part of the drought period (63 days) (Figure 4). The seemingly stable leaf water status along with no apparent up-regulation of SS_N (Figure 4a) suggest a lack of osmotic adjustment with decreasing water availability, controversial to the general drought response of plants (Adams et al., 2017; Li et al., 2018). However, decreasing St_N concentrations indicate the remobilization of starch reserves in *P. halepensis* seedlings in order to meet C requirements when drought response reduces C assimilation (Martínez-Vilalta et al., 2016). A more detailed look at the primary metabolome, but excluding starch, of *P. halepensis* seedlings subjected to heat and hot drought stress revealed that eCO_2 enhanced root protein stability at high temperatures, but did not alter the general stress response (Birami et al., 2020). Contrary to our expectations, eCO_2 trees did apparently not benefit from enhanced NSC reserves. NSC patterns were rather similar between a slow and a fast drought as relations between SS_N/St_N ratios and Ψ_{md} show (Figure 5), emphasizing the complex as well as versatile use of NSC in response to drought.

4.3 | [CO_2] effect on tipping points and drought-induced mortality

In response to severe drought, *P. halepensis* seedlings kept stomata closed but still lost water through cuticular conductance and stomatal leakiness (Blackman et al., 2016). During such conditions, survival depends on both C accessibility, required for instance for metabolic processes such as respiration, and the integrity of the plants hydraulic functions ensuring the maintenance of capacitance and conservation of water storage (Adams et al., 2017; Blackman et al., 2019; Choat et al., 2018; Nardini, Battistuzzo, & Savi, 2013; Sevanto, 2018; Sevanto et al., 2014; Zhu et al., 2018). Regarding C availability under severe drought, non-structural carbohydrates (NSC) have been identified as a key C source (Galiano, Martínez-Vilalta, & Lloret, 2011; Garcia-Forner, Sala, Biel, Savé, & Martínez-Vilalta, 2016; O'Brien, Leuzinger, Philipson, Tay, & Hector, 2014).

However, because of their various functions in plant C metabolism it has been proven to be extremely difficult to specify a particular NSC threshold below which death is more likely than survival (Adams et al., 2017; McDowell et al., 2013; Meir, Mencuccini, & Dewar, 2015). In a global synthesis, Martínez-Vilalta et al. (2016) found a 54 % NSC loss as an overall estimate for minimum NSC in dying relative to control trees. Applied to our SS_N and St_N measurements, the NSC_{50} threshold underlines the mitigating effect of eCO_2 on St_N depletion (Figure 6d). However, due to the uncertainty regarding this threshold we also considered the transition from positive to negative C balance (after growth ceases) as a critical threshold. Since we estimated the C balance as $A_{net,\ canopy}$ minus the sum of shoot and root respiration (R_{total}), a negative C balance means that reductions in $A_{net,\ canopy}$ exceed decreases in R_{total} under declining water availability (Figure 2) further suggesting the requirement for alternative C sources namely NSC. Mitchell, O'Grady, Tissue, Worledge, and Pinkard (2014) attributed importance to Ψ_{md} values between −1.4 and −1.5 MPa by proposing the phase between the cessation of growth and assimilation as a carbon safety margin for isohydric tree species. Since this attempt at defining a carbon safety margin is very rare due to the complex and diverse functions of NSC, the applicability of this approach remains questionable. However, in our study a similar Ψ_{md} range (between −1.4 and −1.6 MPa) delimitated the crucial period beyond which growth must have ceased (net C uptake zero), shortly before the C balance turned negative and stress turned from mild to severe. We found eCO_2 to not affect this carbon safety margin.

In order to assess the risk of dehydration and hydraulic failure under drought, leaf turgor and xylem conductivity are considered as crucial traits (Körner, 2019). Losses in conductivity are strongly linked to xylem cavitation and embolisms indicating a rising possibility of hydraulic dysfunction and ultimately tree mortality (Breshears et al., 2018; Cochard, 2006; Klein et al., 2016; Klein, Cohen, & Yakir, 2011). Irrespective of [CO_2], the TLP of *P. halepensis* seedlings was reached at 80 % RLWC and a Ψ_{md} of −2.2 MPa, which is in line with findings by Villar-Salvador, Ocaña, Peñuelas, and Carrasco (1999) and Royo, Gil, and Pardos (2001). Beyond the TLP, seedlings dehydrated at a fast rate and RLWC was as low as 30 % at mortality. Substantial xylem embolism must have occurred alongside dehydration and a 50 % percentage loss of xylem conductance (PLC50) was reached at Ψ_{md} of about −5 MPa (Gleason et al., 2016) concordant with other PLC50 results for *P. halepensis* (Martin-StPaul, Delzon, & Cochard, 2017).

In previous studies, PLC50 to PLC80 was suggested as the likely critical threshold between survival and death in gymnosperms (Brodribb & Cochard, 2009; Choat et al., 2018; Hammond et al., 2019). All of our seedlings were well beyond a Ψ_{md} related to PLC50, when mortality was reached, indicating that PLC80 might be a more meaningful threshold for mortality in Aleppo pine. In addition, our findings indicate that eCO_2 altered neither the hydraulic thresholds directly, nor the time to reach the lethal hydraulic thresholds (Ψ_{md} did not differ between treatments). This corroborates the surmise that the detected water savings on leaf level are counterbalanced by the leaf area increase in *P. halepensis* seedlings under eCO_2. A similar lack of a [CO_2] effect on whole tree water relations and drought-induced mortality was reported by Duan et al. (2014) for *Eucalyptus radiata* and *Pinus radiata* as well as *Callitris rhomboidea* (Duan et al., 2015). As critical hydraulic thresholds were reached earlier than NSC thresholds, our results indicate that the water status is more meaningful than the C status for predicting mortality risks of *P. halepensis* seedlings under severe drought conditions. This in turn is consistent with findings by Duan et al. (2018) suggesting that predicting time-to-mortality for *Eucalyptus sideroxylon* is better based on leaf water potential than C status. In summary our results further support dehydration as the main cause of death in our seedlings and that eCO_2 did not alter dehydration rates.

Since our study was conducted on potted seedlings in a controlled greenhouse how meaningful are our results for the future of Aleppo pines in the Yatir forest? [CO_2]-stimulated root growth may expand the root zone, which may open up new water sources for the trees. This could be advantageous as our study shows that trees under eCO_2, despite a larger leaf area, transpire the same amount of water on the whole tree level due to reduced stomatal conductance. Together with larger C reserves, this in turn could influence the fate of the trees during drought conditions in favor of their survival. However, predicted reductions in precipitation for the Mediterranean region (Giorgi & Lionello, 2008) alongside new evidence finding allocation changes under eCO_2 to increase leaf area compared to water supplying sapwood area (Trugman et al., 2019), calls into question the potential advantage just described. In combination with an overall absence of [CO_2] interacting with three critical drought thresholds, we conclude that eCO_2 will not improve survival of Aleppo pine seedlings under severe drought. Moreover, a larger non-structural carbohydrate buffer under eCO_2 seemed of no advantage neither during fast nor slow terminal drought, which clearly challenges the carbon starvation hypothesis.

ACKNOWLEDGMENTS

We would like to thank especially Andreas Gast, Andrea-Livia Jakab and Johanna Schnurr for assistance with the experimental set-up and lab work and we want to thank all colleagues who helped on sampling days.

This study was supported by the German Research Foundation through its Emmy Noether Program (RU 1657/2-1). We further acknowledge funding from the German Research Foundation through its German-Israeli project cooperation program (CSCHM 2736/2-1) and by the German Federal Ministry of Education and Research (BMBF), through the Helmholtz Association and its research program ATMO.

CONFLICT OF INTEREST

The authors declare no conflict of interest.

ORCID

Marielle Gattmann https://orcid.org/0000-0001-5035-928X
Benjamin Birami https://orcid.org/0000-0002-0142-8418
Daniel Nadal Sala https://orcid.org/0000-0002-0935-6201
Nadine Katrin Ruehr https://orcid.org/0000-0001-5989-7463

REFERENCES

Adams, H. D., Macalady, A. K., Breshears, D. D., Allen, C. D., Stephenson, N. L., Saleska, S. R., … McDowell, N. G. (2010). Climate-Induced Tree Mortality: Earth System Consequences. *Eos, Transactions American Geophysical Union*, *91*, 153–154. http://doi.org/10.1029/2010eo170003.

Adams, H. D., Zeppel, M. J. B., Anderegg, W. R. L., Hartmann, H., Landhäusser, S. M., Tissue, D. T., … McDowell, N. G. (2017). A multi-species synthesis of physiological mechanisms in drought-induced tree mortality. *Nature Ecology & Evolution*, *1*, 1285–1291. https://doi.org/10.1038/s41559-017-0248-x

Ainsworth, E. A., & Long, S. P. (2004). What have we learned from 15 years of free-air CO2 enrichment (FACE)? A meta-analytic review of the responses of photosynthesis, canopy properties and plant production to rising CO_2: Tansley review. *New Phytologist*, *165*, 351–372. https://doi.org/10.1111/j.1469-8137.2004.01224.x

Ainsworth, E. A., & Rogers, A. (2007). The response of photosynthesis and stomatal conductance to rising [CO_2]: Mechanisms and environmental interactions: Photosynthesis and stomatal conductance responses to rising [CO_2]. *Plant, Cell & Environment*, *30*, 258–270. https://doi.org/10.1111/j.1365-3040.2007.01641.x

Allen, C. D., Breshears, D. D., & McDowell, N. G. (2015). On underestimation of global vulnerability to tree mortality and forest die-off from hotter drought in the Anthropocene. *Ecosphere*, *6*, art129. https://doi.org/10.1890/ES15-00203.1

Allen, C. D., Macalady, A. K., Chenchouni, H., Bachelet, D., McDowell, N., Vennetier, M., … Cobb, N. (2010). A global overview of drought and heat-induced tree mortality reveals emerging climate change risks for forests. *Forest Ecology and Management*, *259*, 660–684.

Anderegg, W. R. L., Anderegg, L. D. L., Kerr, K. L., & Trugman, A. T. (2019). Widespread drought-induced tree mortality at dry range edges indicates that climate stress exceeds species' compensating mechanisms. *Global Change Biology*, *25*, 3793–3802. https://doi.org/10.1111/gcb.14771

Apple, M. E., Olszyk, D. M., Ormrod, D. P., Lewis, J., Southworth, D., & Tingey, D. T. (2000). Morphology and stomatal function of Douglas fir needles exposed to climate change: Elevated CO_2 and temperature. *International Journal of Plant Sciences*, *161*, 127–132. https://doi.org/10.1086/314237

Bartlett, M. K., Klein, T., Jansen, S., Choat, B., & Sack, L. (2016). The correlations and sequence of plant stomatal, hydraulic, and wilting responses to drought. *Proceedings of the National Academy of Sciences*, *113*, 13098–13103. https://doi.org/10.1073/pnas.1604088113

Bates, D., Mächler, M., Bolker, B., & Walker, S. (2015). Fitting linear mixed-effects models using lme4. *Journal of Statistical Software*, *67*, http://doi.org/10.18637/jss.v067.i01.

Benner, P., Sabel, P., & Wild, A. (1988). Photosynthesis and transpiration of healthy and diseased spruce trees in the course of three vegetation periods. *Trees*, *2*, 223–232. http://doi.org/10.1007/bf00202377.

Bettarini, I., Vaccari, F. P., & Miglietta, F. (1998). Elevated CO_2 concentrations and stomatal density: Observations from 17 plant species growing in a CO_2 spring in Central Italy. *Global Change Biology*, *4*, 17–22. https://doi.org/10.1046/j.1365-2486.1998.00098.x

Birami, B., Nägele, T., Gattmann, M., Preisler, Y., Gast, A., Arneth, A., & Ruehr, N. K. (2020). Hot drought reduces the effects of elevated CO_2 on tree water-use efficiency and carbon metabolism. *New Phytologist*, *226*, 1607–1621. https://doi.org/10.1111/nph.16471

Blackman, C. J., Creek, D., Maier, C., Aspinwall, M. J., Drake, J. E., Pfautsch, S., … Choat, B. (2019). Drought response strategies and hydraulic traits contribute to mechanistic understanding of plant dry-down to hydraulic failure. *Tree Physiology*, *39*, 910–924. https://doi.org/10.1093/treephys/tpz016

Blackman, C. J., Pfautsch, S., Choat, B., Delzon, S., Gleason, S. M., & Duursma, R. A. (2016). Toward an index of desiccation time to tree mortality under drought: Desiccation time to tree mortality. *Plant, Cell & Environment*, *39*, 2342–2345. https://doi.org/10.1111/pce.12758

Bréda, N., Huc, R., Granier, A., & Dreyer, E. (2006). Temperate forest trees and stands under severe drought: A review of ecophysiological responses, adaptation processes and long-term consequences. *Annals of Forest Science*, *63*, 625–644. https://doi.org/10.1051/forest:2006042

Breshears, D. D., Carroll, C. J. W., Redmond, M. D., Wion, A. P., Allen, C. D., Cobb, N. S., … Newell-Bauer, O. (2018). A dirty dozen ways to die: metrics and modifiers of mortality driven by drought and warming for a tree species. *Frontiers in Forests and Global Change*, *1*, http://doi.org/10.3389/ffgc.2018.00004.

Brodribb, T. J., & Cochard, H. (2009). Hydraulic failure defines the recovery and point of death in water-stressed conifers. *Plant Physiology*, *149*, 575–584. http://doi.org/10.1104/pp.108.129783.

Brodribb, T. J., Powers, J., Cochard, H., & Choat, B. (2020). Hanging by a thread? Forests and drought. *Science*, *368*, 261–266. https://doi.org/10.1126/science.aat7631

Choat, B., Brodribb, T. J., Brodersen, C. R., Duursma, R. A., López, R., & Medlyn, B. E. (2018). Triggers of tree mortality under drought. *Nature*, *558*, 531–539. https://doi.org/10.1038/s41586-018-0240-x

Cochard, H. (2006). Cavitation in trees. *Comptes Rendus Physique*, *7*, 1018–1026. https://doi.org/10.1016/j.crhy.2006.10.012

Collins, M., Knutti, R., Arblaster, J., Dufresne, J.-L., Fichefet, T., Gao, X., … Tett, S. (2013). Long-term climate change: Projections, Commitments and Irreversibility. In T.F. Stocker, D.Qin, G-K. Plattner, M.M.B. Tignor, S.K. Allen, J. Boschung, A. Nauels, Y. Xia, V. Bex & P.M. Midgley (Eds.), *Climate Change 2013 - The Physical Science Basis: Contribution of Working Group I to the Fifth Assessment Reporst of the Intergovermental Panel on Climate Change*, (1029–1136).

Dai, A. (2013). Increasing drought under global warming in observations and models. *Nature Climate Change*, *3*, 52–58. http://doi.org/10.1038/nclimate1633.

Domec, J.-C., Palmroth, S., & Oren, R. (2016). Effects of *Pinus taeda* leaf anatomy on vascular and extravascular leaf hydraulic conductance as influenced by N-fertilization and elevated CO_2. *Journal of Plant Hydraulics*, *3*, e007. https://doi.org/10.20870/jph.2016.e007

Domec, J.-C., Palmroth, S., Ward, E., Maier, C. A., Thérézien, M., & Oren, R. (2009). Acclimation of leaf hydraulic conductance and stomatal conductance of *Pinus taeda* (loblolly pine) to long-term growth in elevated CO_2 (free-air CO_2 enrichment) and N-fertilization. *Plant, Cell & Environment*, *32*, 1500–1512. https://doi.org/10.1111/j.1365-3040.2009.02014.x

Duan, H., Chaszar, B., Lewis, J. D., Smith, R. A., Huxman, T. E., & Tissue, D. T. (2018). CO_2 and temperature effects on morphological and physiological traits affecting risk of drought-induced mortality. *Tree Physiology*, *38*, 1138–1151. https://doi.org/10.1093/treephys/tpy037

Duan, H., Duursma, R. A., Huang, G., Smith, R. A., Choat, B., O'Grady, A. P., & Tissue, D. T. (2014). Elevated [CO_2] does not ameliorate the negative effects of elevated temperature on drought-induced mortality in *E ucalyptus radiata* seedlings: Mortality under rising [CO_2] and temperature. *Plant, Cell & Environment*, *37*, 1598–1613. https://doi.org/10.1111/pce.12260

Duan, H., O'Grady, A. P., Duursma, R. A., Choat, B., Huang, G., Smith, R. A., … Tissue, D. T. (2015). Drought responses of two gymnosperm species with contrasting stomatal regulation strategies under elevated [CO_2] and temperature. *Tree Physiology*, *35*, 756–770. https://doi.org/10.1093/treephys/tpv047

Dusenge, M. E., Duarte, A. G., & Way, D. A. (2019). Plant carbon metabolism and climate change: Elevated CO_2 and temperature impacts on photosynthesis, photorespiration and respiration. *New Phytologist*, *221*, 32–49. https://doi.org/10.1111/nph.15283

Eguchi, N., Fukatsu, E., Funada, R., Tobita, H., Kitao, M., Maruyama, Y., & Koike, T. (2004). Changes in morphology, anatomy, and photosynthetic capacity of needles of Japanese larch (*Larix kaempferi*) seedlings grown in high CO_2 concentrations. *Photosynthetica*, *42*, 173–178. https://doi.org/10.1023/B:PHOT.0000040587.99518.a8

Fensham, R. J., & Holman, J. E. (1999). Temporal and spatial patterns in drought-related tree dieback in Australian savanna. *Journal of Applied Ecology*, *36*, 1035–1050. https://doi.org/10.1046/j.1365-2664.1999.00460.x

Flexas, J. (2002). Drought-inhibition of photosynthesis in C3 plants: stomatal and non-stomatal limitations revisited. *Annals of Botany*, *89*, 183–189. http://doi.org/10.1093/aob/mcf027.

Galiano, L., Martínez-Vilalta, J., & Lloret, F. (2011). Carbon reserves and canopy defoliation determine the recovery of scots pine 4 yr after a drought episode. *New Phytologist*, *190*, 750–759. https://doi.org/10.1111/j.1469-8137.2010.03628.x

Gamage, D., Thompson, M., Sutherland, M., Hirotsu, N., Makino, A., & Seneweera, S. (2018). New insights into the cellular mechanisms of plant growth at elevated atmospheric carbon dioxide concentrations: Elevated CO_2 effect on plant growth and development. *Plant, Cell & Environment*, *41*, 1233–1246. https://doi.org/10.1111/pce.13206

Garcia-Forner, N., Sala, A., Biel, C., Savé, R., & Martínez-Vilalta, J. (2016). Individual traits as determinants of time to death under extreme drought in *Pinus sylvestris* L. *Tree Physiology*, *36*, 1196–1209. https://doi.org/10.1093/treephys/tpw040

Giorgi, F., & Lionello, P. (2008). Climate change projections for the Mediterranean region. *Global and Planetary Change*, *63*, 90–104. https://doi.org/10.1016/j.gloplacha.2007.09.005

Gleason, S. M., Westoby, M., Jansen, S., Choat, B., Hacke, U. G., Pratt, R. B., … Zanne, A. E. (2016). Weak tradeoff between xylem

safety and xylem-specific hydraulic efficiency across the world's woody plant species. *New Phytologist*, *209*, 123–136. http://doi.org/10.1111/nph.13646.

Greer, D. H. (2019). Limitations to photosynthesis of leaves of apple (*Malus domestica*) trees across the growing season prior to and after harvest. *Photosynthetica*, *57*, 483–490. https://doi.org/10.32615/ps.2019.063

Grunzweig, J. M., Lin, T., Rotenberg, E., Schwartz, A., & Yakir, D. (2003). Carbon sequestration in arid-land forest. *Global Change Biology*, *9*, 791–799. https://doi.org/10.1046/j.1365-2486.2003.00612.x

Hammond, W. M., & Adams, H. D. (2019). Dying on time: Traits influencing the dynamics of tree mortality risk from drought. *Tree Physiology*, *39*, 906–909. https://doi.org/10.1093/treephys/tpz050

Hammond, W. M., Yu, K., Wilson, L. A., Will, R. E., Anderegg, W. R. L., & Adams, H. D. (2019). Dead or dying? Quantifying the point of no return from hydraulic failure in drought-induced tree mortality. *New Phytologist*, *223*, 1834–1843. https://doi.org/10.1111/nph.15922

Hartmann, H. (2015). Carbon starvation during drought-induced tree mortality – Are we chasing a myth? *Journal of Plant Hydraulics*, *2*, e005. https://doi.org/10.20870/jph.2015.e005

Hartmann, H., Moura, C. F., Anderegg, W. R. L., Ruehr, N. K., Salmon, Y., Allen, C. D., … O'Brien, M. (2018). Research frontiers for improving our understanding of drought-induced tree and forest mortality. *New Phytologist*, *218*, 15–28. https://doi.org/10.1111/nph.15048

Hausfather, Z., & Peters, G. P. (2020). Emissions – The 'business as usual' story is misleading. *Nature*, *577*, 618–620. https://doi.org/10.1038/d41586-020-00177-3

Haworth, M., Heath, J., & McElwain, J. C. (2010). Differences in the response sensitivity of stomatal index to atmospheric CO2 among four genera of Cupressaceae conifers. *Annals of Botany*, *105*, 411–418. https://doi.org/10.1093/aob/mcp309

Hlásny, T., Trombik, J., Bošeľa, M., Merganič, J., Marušák, R., Šebeň, V., … Trnka, M. (2017). Climatic drivers of forest productivity in Central Europe. *Agricultural and Forest Meteorology*, *234-235*, 258–273. http://doi.org/10.1016/j.agrformet.2016.12.024.

Hsiao, T. C. (1973). Plant Responses to Water Stress. *Annual Review of Plant Physiology*, *24*, 519–570. http://doi.org/10.1146/annurev.pp.24.060173.002511.

Huang, J., Yu, H., Guan, X., Wang, G., & Guo, R. (2016). Accelerated dryland expansion under climate change. *Nature Climate Change*, *6*, 166–171. http://doi.org/10.1038/nclimate2837.

Hui, D., Deng, Q., Tian, H., & Luo, Y. (2017). Climate change and carbon sequestration in Forest ecosystems. In W.-Y. Chen, T. Suzuki, & M. Lackner (Eds.), *Handbook of Climate Change Mitigation and Adaptation* (pp. 555–594). Switzerland: Springer Nature.

IPCC (2014). In C. W. Team, R. K. Pachauri, & L. A. Meyer (Eds.), *Climate Change 2014: Synthesis Report. Contribution of Working Groups I, II and III to the Fifth Assessment Report of the Intergovernmental Panel on Climate Change*. Geneva, Switzerland: IPCC.

Je, S., Woo, S. Y., Lee, S. H., Kwak, M. J., Lee, T. Y., & Kim, S. H. (2018). Combined effect of elevated CO_2 concentration and drought on the photosynthetic apparatus and leaf morphology traits in seedlings of yellow poplar. *Ecological Research*, *33*, 403–412. https://doi.org/10.1007/s11284-017-1495-7

Jin, Z., Ainsworth, E. A., Leakey, A. D. B., & Lobell, D. B. (2018). Increasing drought and diminishing benefits of elevated carbon dioxide for soybean yields across the US Midwest. *Global Change Biology*, *24*, e522–e533. https://doi.org/10.1111/gcb.13946

Klein, T., Cohen, S., Paudel, I., Preisler, Y., Rotenberg, E., & Yakir, D. (2016). Diurnal dynamics of water transport, storage and hydraulic conductivity in pine trees under seasonal drought. *IForest – Biogeosciences and Forestry*, *9*, 710–719. https://doi.org/10.3832/ifor2046-009

Klein, T., Cohen, S., & Yakir, D. (2011). Hydraulic adjustments underlying drought resistance of *Pinus halepensis*. *Tree Physiology*, *31*, 637–648. https://doi.org/10.1093/treephys/tpr047

Knauer, J., Zaehle, S., Reichstein, M., Medlyn, B. E., Forkel, M., Hagemann, S., & Werner, C. (2017). The response of ecosystem water-use efficiency to rising atmospheric CO_2 concentrations: Sensitivity and large-scale biogeochemical implications. *New Phytologist*, *213*, 1654–1666. https://doi.org/10.1111/nph.14288

Körner, C. (2019). No need for pipes when the well is dry—A comment on hydraulic failure in trees. *Tree Physiology*, *39*, 695–700. https://doi.org/10.1093/treephys/tpz030

Kuznetsova, A., Brockhoff, P. B., & Christensen, R. H. B. (2017). lmerTest package: tests in linear mixed effects models. *Journal of Statistical Software*, *82*, http://doi.org/10.18637/jss.v082.i13.

Landhäusser, S. M., Chow, P. S., Dickman, L. T., Furze, M. E., Kuhlman, I., Schmid, S., … Adams, H. D. (2018). Standardized protocols and procedures can precisely and accurately quantify non-structural carbohydrates. *Tree Physiology*, *38*, 1764–1778. https://doi.org/10.1093/treephys/tpy118

Lavergne, A., Graven, H., De Kauwe, M. G., Keenan, T. F., Medlyn, B. E., & Prentice, I. C. (2019). Observed and modelled historical trends in the water-use efficiency of plants and ecosystems. *Global Change Biology*, *25*, 2242–2257. http://doi.org/10.1111/gcb.14634.

Lenth, R. (2019). emmeans: Estimated Marginal Means, aka Least-Squares Means. R package version 1.3.2.

Li, W., Hartmann, H., Adams, H. D., Zhang, H., Jin, C., Zhao, C., … Wu, J. (2018). The sweet side of global change–dynamic responses of non-structural carbohydrates to drought, elevated CO2 and nitrogen fertilization in tree species. *Tree Physiology*, *38*, 1706–1723. http://doi.org/10.1093/treephys/tpy059.

Liu, S., Bond-Lamberty, B., Boysen, L. R., Ford, J. D., Fox, A., Gallo, K., … Zhao, S. (2017). Grand challenges in understanding the interplay of climate and land changes. *Earth Interactions*, *21*, 1–43. https://doi.org/10.1175/EI-D-16-0012.1.

Mackay, D. S., Roberts, D. E., Ewers, B. E., Sperry, J. S., McDowell, N. G., & Pockman, W. T. (2015). Interdependence of chronic hydraulic dysfunction and canopy processes can improve integrated models of tree response to drought: Modeling chronic hydraulic dysfunction and canopy processes. *Water Resources Research*, *51*, 6156–6176. https://doi.org/10.1002/2015WR017244

Martínez-Vilalta, J., Sala, A., Asensio, D., Galiano, L., Hoch, G., Palacio, S., … Lloret, F. (2016). Dynamics of non-structural carbohydrates in terrestrial plants: A global synthesis. *Ecological Monographs*, *86*, 495–516. https://doi.org/10.1002/ecm.1231

Martin-StPaul, N., Delzon, S., & Cochard, H. (2017). Plant resistance to drought depends on timely stomatal closure. *Ecology Letters*, *20*, 1437–1447. https://doi.org/10.1111/ele.12851

Maruyama, Y., Nakamura, S., Marenco, R. A., Vieira, G., & Sato, A. (2005). Photosynthetic traits of seedlings of several tree species in an Amazonian forest. *Tropics*, *14*, 211–219. https://doi.org/10.3759/tropics.14.211

McDowell, N., Pockman, W. T., Allen, C. D., Breshears, D. D., Cobb, N., Kolb, T., … Yepez, E. A. (2008). Mechanisms of plant survival and mortality during drought: Why do some plants survive while others succumb to drought? *New Phytologist*, *178*, 719–739. https://doi.org/10.1111/j.1469-8137.2008.02436.x

McDowell, N. G., Fisher, R. A., Xu, C., Domec, J. C., Hölttä, T., Mackay, D. S., … Pockman, W. T. (2013). Evaluating theories of drought-induced vegetation mortality using a multimodel-experiment framework. *New Phytologist*, *200*, 304–321. https://doi.org/10.1111/nph.12465

Meir, P., Mencuccini, M., & Dewar, R. C. (2015). Drought-related tree mortality: Addressing the gaps in understanding and prediction. *New Phytologist*, *207*, 28–33. https://doi.org/10.1111/nph.13382

Mitchell, P. J., O'Grady, A. P., Tissue, D. T., White, D. A., Ottenschlaeger, M. L., & Pinkard, E. A. (2013). Drought response strategies define the relative contributions of hydraulic dysfunction and carbohydrate depletion during tree mortality. *New Phytologist*, *197*, 862–872. https://doi.org/10.1111/nph.12064

Mitchell, P. J., O'Grady, A. P., Tissue, D. T., Worledge, D., & Pinkard, E. A. (2014). Co-ordination of growth, gas exchange and hydraulics define the carbon safety margin in tree species with contrasting drought strategies. *Tree Physiology*, *34*, 443–458. https://doi.org/10.1093/treephys/tpu014

Mount, J., & Zumel, N. (2019). sigr: Succinct and Correct Statistical Summaries for Reports. R package version 1.0.6.

Nabuurs, G. J., Hengeveld, G. M., van der Werf, D. C., & Heidema, A. H. (2010). European forest carbon balance assessed with inventory based methods—An introduction to a special section. *Forest Ecology and Management*, *260*, 239–240. http://doi.org/10.1016/j.foreco.2009.11.024.

Nardini, A., Battistuzzo, M., & Savi, T. (2013). Shoot desiccation and hydraulic failure in temperate woody angiosperms during an extreme summer drought. *New Phytologist*, *200*, 322–329. https://doi.org/10.1111/nph.12288

Niu, S., Luo, Y., Li, D., Cao, S., Xia, J., Li, J., & Smith, M. D. (2014). Plant growth and mortality under climatic extremes: An overview. *Environmental and Experimental Botany*, *98*, 13–19. https://doi.org/10.1016/j.envexpbot.2013.10.004.

O'Brien, M. J., Engelbrecht, B. M. J., Joswig, J., Pereyra, G., Schuldt, B., Jansen, S., … Macinnis-Ng, C. (2017). A synthesis of tree functional traits related to drought-induced mortality in forests across climatic zones. *Journal of Applied Ecology*, *54*, 1669–1686. https://doi.org/10.1111/1365-2664.12874

O'Brien, M. J., Leuzinger, S., Philipson, C. D., Tay, J., & Hector, A. (2014). Drought survival of tropical tree seedlings enhanced by non-structural carbohydrate levels. *Nature Climate Change*, *4*, 710–714. https://doi.org/10.1038/nclimate2281

Phillips, O. L., van der Heijden, G., Lewis, S. L., López-González, G., Aragão, L. E. O. C., Lloyd, J., … Vilanova, E. (2010). Drought-mortality relationships for tropical forests. *New Phytologist*, *187*, 631–646. https://doi.org/10.1111/j.1469-8137.2010.03359.x

Poorter, H., Van Berkel, Y., Baxter, R., Den Hertog, J., Dijkstra, P., Gifford, R. M., … Wong, S. C. (1997). The effect of elevated CO_2 on the chemical composition and construction costs of leaves of 27 C3 species. *Plant, Cell & Environment*, *20*, 472–482. https://doi.org/10.1046/j.1365-3040.1997.d01-84.x

Preisler, Y., Tatarinov, F., Grünzweig, J. M., Bert, D., Ogée, J., Wingate, L., … Yakir, D. (2019). Mortality versus survival in drought-affected Aleppo pine forest depends on the extent of rock cover and soil stoniness. *Functional Ecology*, *33*, 901–912. https://doi.org/10.1111/1365-2435.13302

Pritchard, S. G., Rogers, H. H., Prior, S. A., & Peterson, C. M. (1999). Elevated CO_2 and plant structure: A review. *Global Change Biology*, *5*, 807–837. https://doi.org/10.1046/j.1365-2486.1999.00268.x

Pushnik, J. C., Demaree, R. S., Houpis, J. L. J., Flory, W. B., Bauer, S. M., & Anderson, P. D. (1995). The Effect of Elevated Carbon Dioxide on a Sierra-Nevadan Dominant Species: Pinus ponderosa. *Journal of Biogeography*, *22*, 249–254. http://doi.org/10.2307/2845918.

Reichstein, M., Bahn, M., Ciais, P., Frank, D., Mahecha, M. D., Seneviratne, S. I., … Wattenbach, M. (2013). Climate extremes and the carbon cycle. *Nature*, *500*, 287–295. http://doi.org/10.1038/nature12350.

Rennenberg, H., Loreto, F., Polle, A., Brilli, F., Fares, S., Beniwal, R. S., & Gessler, A. (2006). Physiological responses of forest trees to heat and drought. *Plant Biology*, *8*, 556–571. https://doi.org/10.1055/s-2006-924084

Resco, V., Ewers, B. E., Sun, W., Huxman, T. E., Weltzin, J. F., & Williams, D. G. (2009). Drought-induced hydraulic limitations constrain leaf gas exchange recovery after precipitation pulses in the C_3 woody legume, *Prosopis velutina*. *New Phytologist*, *181*, 672–682. https://doi.org/10.1111/j.1469-8137.2008.02687.x

Roberntz, P., & Stockfors, J. (1998). Effects of elevated CO2 concentration and nutrition on net photosynthesis, stomatal conductance and needle respiration of field-grown Norway spruce trees. *Tree Physiology*, *18*, 233–241. https://doi.org/10.1093/treephys/18.4.233

Robredo, A., Pérez-López, U., Lacuesta, M., Mena-Petite, A., & Muñoz-Rueda, A. (2010). Influence of water stress on photosynthetic characteristics in barley plants under ambient and elevated CO_2 concentrations. *Biologia Plantarum*, *54*, 285–292. https://doi.org/10.1007/s10535-010-0050-y

Royo, A., Gil, L., & Pardos, J. A. (2001). Effect of water stress conditioning on morphology, physiology and field performance of *Pinus halepensis* mill seedlings. *New Forests*, *21*, 127–140. https://doi.org/10.1023/A:1011892732084

Ruehr, N. K., Grote, R., Mayr, S., & Arneth, A. (2019). Beyond the extreme: Recovery of carbon and water relations in woody plants following heat and drought stress. *Tree Physiology*, *39*, 1285–1299. https://doi.org/10.1093/treephys/tpz032

Ryan, M. G. (2011). Tree responses to drought. *Tree Physiology*, *31*, 237–239. https://doi.org/10.1093/treephys/tpr022

Sáenz-Romero, C., Larter, M., González-Muñoz, N., Wehenkel, C., Blanco-Garcia, A., Castellanos-Acuña, D., Burlett, R., & Delzon, S. (2017). Mexican conifers differ in their capacity to face climate change. *Journal of Plant Hydraulics*, *4*, http://doi.org/10.20870/jph.2017.e003.

Saurer, M., Siegwolf, R. T. W., & Schweingruber, F. H. (2004). Carbon isotope discrimination indicates improving water-use efficiency of trees in northern Eurasia over the last 100 years. *Global Change Biology*, *10*, 2109–2120. https://doi.org/10.1111/j.1365-2486.2004.00869.x

Sevanto, S. (2018). Drought impacts on phloem transport. *Current Opinion in Plant Biology*, *43*, 76–81. https://doi.org/10.1016/j.pbi.2018.01.002

Sevanto, S., Mcdowell, N. G., Dickman, L. T., Pangle, R., & Pockman, W. T. (2014). How do trees die? A test of the hydraulic failure and carbon starvation hypotheses. *Plant, Cell & Environment*, *37*, 153–161. https://doi.org/10.1111/pce.12141

Sperlich, D., Chang, C. T., Penuelas, J., Gracia, C., & Sabate, S. (2015). Seasonal variability of foliar photosynthetic and morphological traits and drought impacts in a Mediterranean mixed forest. *Tree Physiology*, *35*, 501–520. https://doi.org/10.1093/treephys/tpv017

Taïbi, K., del Campo, A. D., Vilagrosa, A., Bellés, J. M., López-Gresa, M. P., Pla, D., … Mulet, J. M. (2017). Drought tolerance in *Pinus halepensis* seed sources as identified by distinctive physiological and molecular markers. *Frontiers in Plant Science*, *8*. https://doi.org/10.3389/fpls.2017.01202

Tatarinov, F., Rotenberg, E., Maseyk, K., Ogée, J., Klein, T., & Yakir, D. (2016). Resilience to seasonal heat wave episodes in a Mediterranean pine forest. *New Phytologist*, *210*, 485–496. https://doi.org/10.1111/nph.13791

Tor-ngern, P., Oren, R., Ward, E. J., Palmroth, S., McCarthy, H. R., & Domec, J.-C. (2015). Increases in atmospheric CO_2 have little influence on transpiration of a temperate forest canopy. *New Phytologist*, *205*, 518–525. https://doi.org/10.1111/nph.13148

Trugman, A. T., Anderegg, L. D. L., Wolfe, B. T., Birami, B., Ruehr, N. K., Detto, M., … Anderegg, W. R. L. (2019). Climate and plant trait strategies determine tree carbon allocation to leaves and mediate future forest productivity. *Global Change Biology*, *25*, 3395–3405. https://doi.org/10.1111/gcb.14680

Villar-Salvador, P., Ocaña, L., Peñuelas, J., & Carrasco, I. (1999). Effect of water stress conditioning on the water relations, root growth capacity, and the nitrogen and non-structural carbohydrate concentration of Pinus halepensis Mill. (Aleppo pine) seedlings. *Annals of Forest Science*, *56*, 459–465. http://doi.org/10.1051/forest:19990602.

Wullschleger, S. D., Tschaplinski, T. J., & Norby, R. J. (2002). Plant water relations at elevated CO_2—Implications for water-limited environments. *Plant, Cell & Environment*, *25*, 319–331. https://doi.org/10.1046/j.1365-3040.2002.00796.x

Xu, Z., Jiang, Y., Jia, B., & Zhou, G. (2016). Elevated-CO_2 response of stomata and its dependence on environmental factors. *Frontiers in Plant Science*, *7*. https://doi.org/10.3389/fpls.2016.00657

Zhu, S.-D., Chen, Y.-J., Ye, Q., He, P.-C., Liu, H., Li, R.-H., … Cao, K.-F. (2018). Leaf turgor loss point is correlated with drought tolerance and leaf carbon economics traits. *Tree Physiology*, *38*, 658–663. https://doi.org/10.1093/treephys/tpy013

SUPPORTING INFORMATION

Additional supporting information may be found online in the Supporting Information section at the end of this article.

How to cite this article: Gattmann M, Birami B, Nadal Sala D, Ruehr NK. Dying by drying: Timing of physiological stress thresholds related to tree death is not significantly altered by highly elevated CO_2. *Plant Cell Environ*. 2021;44:356–370. https://doi.org/10.1111/pce.13937